Colloid Polym Sci (2007) 285:729–736
DOI 10.1007/s00396-006-1622-4

ORIGINAL CONTRIBUTION

Functionalization of silicon nanoparticles via hydrosilylation with 1-alkenes

Jürgen Nelles · Dorota Sendor · Andre Ebbers · Frank Martin Petrat · Hartmut Wiggers · Christof Schulz · Ulrich Simon

Received: 20 October 2006 / Accepted: 7 November 2006 / Published online: 20 January 2007

Abstract Studies focusing on the functionalization of the surface of free silicon nanoparticles are presented. This functionalization is applied to hydrogen-terminated silicon nanoparticles to evaluate how far the well-known solution-phase chemistry of thermal-, radical-, Lewis acid- and UV light-mediated hydrosilylation can be applied to the surface chemistry of silicon nanoparticles. The efficiencies of hydrosilylation for thermal-, radical- and Lewis acid-mediated reactions on silicon nanoparticles surfaces, deduced from the intensity of the ν(Si–H) absorption, are found to be comparable.

Keywords Hydrosilylation · Silicon nanoparticles · Surface functionalization

Introduction

Silicon is one of the technologically most important materials utilized today owing to its ubiquitous role in microelectronic compounds. The chemical nature of silicon interface atoms plays a crucial role in the proper performance and characteristics of an electronic device. Whereas thermal oxide on silicon has been proven to be extremely useful in electronically passivating of bulk silicon, much attention is being directed towards the synthesis of organic monolayers on silicon, which can be modified upon demand for specific requirements [1]. By tapping into the vast resources of organic chemistry, a wide variety of surface functionalities can be achieved, which will allow fine tuning of surface characteristics for a broad range of applications, e.g. optoelectronics [2]. However, oxidation of the surface is not desirable for many applications. For example, the electroluminescence efficiency can be reduced if luminescent silicon nanoparticles are covered with an insulating oxide layer [2]. For sensor applications, attachment of chemical species is desired to impart specificity [3]. This can be accomplished through alkoxide or ester linkages, although the Si–O bond in this case is readily hydrolyzed, limiting the stability and applicability [4]. Thus, it is highly desirable to prepare silicon surfaces with well-defined and variable chemical characteristics that are chemically stable. Therefore, several different approaches have been made to first evaluate the surface reactivity of non-oxidized silicon and then, to subsequently exploit the reactivity to prepare stable, functional interfaces. In this case, non-oxidized means that the surface has not reacted with oxygen, independently from the fact that the silicon atoms at the particles' surface are formally not in the oxidation stage zero (like in Si–H). So in the following, the term oxidation has more of the meaning of oxygenation, i.e. the reaction with oxygen, than the meaning of a formal change of the oxidation stage.

For the preparation of functionalized, non-oxidized silicon surfaces, hydrogen-terminated silicon surfaces generally

J. Nelles · D. Sendor · U. Simon (✉)
Institute of Inorganic Chemistry, RWTH Aachen,
Landoltweg 1,
52074 Aachen, Germany
e-mail: ulrich.simon@ac.rwth-aachen.de

A. Ebbers · F. M. Petrat
Degussa AG, Creavis Technologies and Innovation,
Paul-Baumann-Straße 1,
45764 Marl, Germany

H. Wiggers · C. Schulz
Institute of Combustion and Gas Dynamic,
University Duisburg-Essen,
Lotharstrasse 1,
47057 Duisburg, Germany

serve as an ideal starting point. The hydrogen-terminated surfaces are extremely useful surface precursors because the Si–H and Si–Si bonds can serve as chemical handles through which functionalization can be mediated.

A potentially interesting route to equip the silicon surface with environmentally robust organic termini is the hydrosilylation. The body of literature involving functionalization with hydrosilylation of compounds containing soluble, molecular silicon hydride and silicon–silicon is extensive. Several of these reactions for molecular compounds have been adapted to silicon surfaces, both flat wafer and porous silicon. High-quality alkyl monolayers on hydrogen-terminated Si(111) were prepared by Linford et al. [5]. These monolayers were produced by a reaction of 1-alkenes and 1-alkynes with the surface upon free-radical initiation with diacyl peroxides. Similar work was done by Sieval et al. [6] to prepare stable Si–C linked functionalized monolayers on the hydrogen-terminated Si(100) surface. Buriak et al. [7] published a series of works on surface modification of silicon and porous silicon. They coated non-oxidized hydrogen-terminated porous silicon surfaces and the Si (111) surface with alkenyl and alkyl functionalities in the presence of Lewis acid catalysis and studied the photoluminescence of the treated porous silicon. Li et al. [8] presented an amine catalyzed method for carrying out silane chemistry on porous silicon without pretreating the surface with an oxidizer to form Si–OH groups on the surface. Schmelzer et al. [9] prepared an alkenyl- and alkyl-terminated surface by hydride abstraction with triphenylcarbenium cations in the presence of terminal alkenes and alkynes. The preparation of the hydrogen-terminated Si(111) or Si(100) surfaces, the reactions involved formation of Si–O and Si–C bonds and the functionalization of monolayers were reviewed by Wayner and Wolkow [10] and Buriak [11].

Although there have been a huge number of papers published on porous silicon and on the surface chemistry of silicon and flat silicon wafer surfaces, however, the knowledge of the surface chemistry of silicon nanoparticles that are free of a substrate and that have not been derived from porous silicon is scanty. Therefore, we focused, in this study, on the functionalization of the surface of free silicon hydrogen-terminated nanoparticles. We compared different methods, i.e. hydrosilylation of 1-alkene by thermal, radical, Lewis acid or UV light mediation in solution, to evaluate the efficiency of respective functionalization processes.

Experimental section

Material fabrication

Silicon nanoparticles were produced by pyrolysis of silane diluted in argon in a hot wall gasphase reactor [12].

Chemical modification

All chemicals were reagent grade or the highest available commercial grade and used as received, unless otherwise specified. All procedures were carried out in an argon atmosphere in Teflon vessels (Bolender), unless otherwise specified.

One-pot route In a typical experiment, 40 ml of hydrofluoric acid (40%, Merck) was added to 40 ml of a silicon nanoparticle suspension (3% in ethanol) and stirred for 30 min. For the thermal modification, 80 ml of the reagent (e.g. 1-octene) was added. After the reaction time, while the vessel is heated in an oil bath, the two phases are separated. For the catalytic modification, first the hydrofluoric acid was removed by heating, and then 80 ml of the reagent with the catalyst within was added. As catalyst, we used dibenzoylperoxide (Fluka), Karstedt-catalyst (platinum-1,3-divinyl-1,1,3,3-tetramethyldisiloxan-complex in xylene, KMF), triphenylcarbenium-tetrakis(pentafluorophenyl)borate (Across) and triphenylcarbenium-tetrafluoroborate (Across). While the reaction time the vessel is heated in an oil bath.

Two-pot route In a typical experiment, 40 ml of hydrofluoric acid (40%, Merck) was added to 40 ml of a silicon nanoparticle suspension (3% in ethanol) and stirred for 30 min. Eighty millilitres of the extracting agent was added and the two phases were separated subsequently. For the thermal modification, 80 ml of the reagent (e.g. 1-octene) was added to the organic phase. For the catalytic modification, 80 ml of the reagent with the catalyst within was added to the organic phase. While the reaction time the vessel is heated in an oil bath, respectively. For the photochemical modification, 80 ml of the reagent and the organic phase was irradiated in a quartz vessel. As a UV light source, we used a 150-W Hg lamp.

To isolate the nanoparticles, the suspension was filtered with a polytetrafluoroethylene filter and washed with *n*-pentane. The product was dried in vacuum at 120 °C and stored in air.

Spectroscopic characterization

Diffuse reflectance infrared Fourier transform (DRIFT) spectra were recorded on a Nicolet 360 Fourier transform infrared (FTIR) spectrometer. Fifty scans were accumulated with a typical spectral resolution of 2 cm^{-1}. The Omic 5.1 software package was used for acquisition of data.

Results and discussion

Under ambient conditions in air, oxidation of the nanoparticles' surface is observed as shown in the DRIFT spectrum in Fig. 1 (solid line).

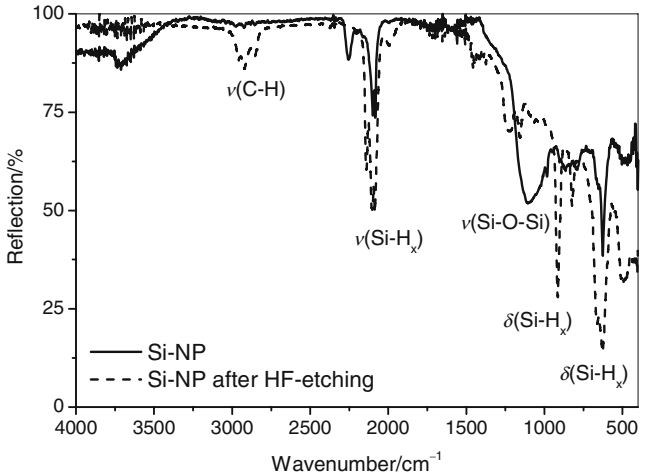

Fig. 1 DRIFT spectra of silicon nanoparticles before (*solid line*) and after etching for 30 min in 24% hydrofluoric acid (*dashed line*)

Besides the signals expected for δ(Si–H) between 800 and 960 cm^{-1} and ν(Si–H) at 2,100 cm^{-1} signals originating from ν(Si–O) between 1,000 and 1,100 cm^{-1}, ν[(O_3)Si–H] at 2,272 cm^{-1} and ν(Si–OH) at 3,650 cm^{-1} have been detected. Preparation of hydrogen-terminated silicon nanoparticle surfaces took advantage of the known reactions of aqueous hydrofluoric acid solution with silicon. On flat silicon wafers, one can readily generate Si–H surfaces with excellent chemical homogeneity (>99% hydrogen termination) by using hydrofluoric acid [13]. We have used the same method to produce hydrogen-terminated nanoparticle surfaces and stirred silicon nanoparticles in 24% hydrofluoric acid for 30 min in the presence of *n*-dodecane. The FTIR spectrum of freshly etched silicon nanoparticles (Fig. 1, dashed line) displays absorption characteristic of surface ν(Si–H), ν(Si–H_2) and ν(Si–H_3) species at 2,086, 2,100 and 2,140 cm^{-1}, respectively [14]. The high surface area of silicon nanoparticles is terminated after etching with hydrofluoric acid with ν(Si–H_x; x=1, 2, 3) bonds without any preferred species, in contrast to crystalline Si(111) surfaces, where Si–H_1 species appear after etching with NH_4F or by Si(100) surface, and where Si–H_2 species appear after etching with hydrofluoric acid [15]. A weak signal at 1,060 cm^{-1} (as compared to starting material) in Fig. 1b is probably due to interstitial oxygen in the silicon lattice because the broad band associated with adsorbed water at 3,500–3,600 cm^{-1} has vanished. This indicates that the surface is now hydrophobic, supported by the fact that the particles spontaneously transfer into hydrophobic organic solvents, e.g. *n*-dodecane. After drying 2 h at 120 °C in vacuum, an absorption with small intensity corresponding to ν(C–H) from the solvent is still visible in Fig. 1. These particles are then used for further surface treatment to generate the functionalized surface with 1-alkenes. The Si–H passivation is only metastable with respect to oxidation under ambient conditions, thus excluding long-term use in most cases. These surfaces can, however, be handled in air for few days with only a little degradation due to kinetic stabilization. Hydrogen-terminated nanoparticles in *n*-dodecane were transferred to a flask and mixed with additional 1-alkene. Table 1 displays the reactivity of the hydrogen-terminated silicon nanoparticles with 1-octene obtain from the different hydrosilylation methods; i.e. samples A and F with thermal treatment, sample B with platinum-1,3-divinyl-1,1,3,3-tetramethyldisiloxan-complex (platinum catalyst), sample C with triphenylcarbenium-tetrakis(pentafluorophenyl)borate (Ph_3C^+), sample D with *N*,*N*-Azobisisobutyronitrile (AIBN) and sample E using UV light, respectively.

Each reaction was carried out for 4 h. The reaction product was washed with pentane and dried 2 h at 120 °C in vacuum. The intensity of the ν(Si–H_x) region decreased in all cases after hydrosilylation, indicating consumption of Si–H bonds at the surface in favour of the covalent attachment of the hydrocarbon. The absorption intensity of Si–H_x stretching modes can therefore be used as a relative index of the reaction progress. Hence, we determined the efficiency E_h of the hydrosilylation from the change in the integrated intensity A of the Si–H absorption (2,000–2,200 cm^{-1}): $E_h = (A_0 - A_1)/A_0$, where A_0 and A_1 are the baseline to peak areas of the reference sample and the hydrosilylated sample, respectively [16]. The intensity ratio I(Si–O)/I(Si–H) of ν(Si–O) at 1,096 cm^{-1} and ν(Si–H) at 2,100 cm^{-1} is also noted because oxidation could be a concurrent reaction to hydrosilylation.

The DRIFT spectra of hydrosilylation mediated thermally (Fig. 2a), by platinum complexes (Fig. 2b), by Lewis acid (Fig. 2c), by radical initiator (Fig. 2d) and by UV light (Fig. 2e) show that in all cases the functionalization of silicon nanoparticles with 1-octene yields alkyl-terminated nanoparticles.

All DRIFT spectra exhibit three close-lying absorption bands centred at 2,900 cm^{-1} and being characteristic for ν(C–H_x) stretching modes. At the same time, physisorption of free alkenes [ν(C=C)=1,650 cm^{-1} or ν(C=CH_2=3,050 cm^{-1}] is not observed, in contrast to a control experiment, where we kept the nanoparticles in the presence of the alkene for the same time at room temperature, and no conversion took place. The data below correspond to 1-octane terminated samples prepared through thermal treatment: ν(CH_3)=2,960 cm^{-1}, ν_{as}=2,922 cm^{-1}, ν_s(CH_2)=2,856 cm^{-1}, ν[(Si_3)Si–H]=2,101 cm^{-1}, δ(CH_2)=1,459 cm^{-1}, δ(CH_3)=1,379 cm^{-1}, ν(Si–O)=1,096 cm^{-1}, δ(SiH_2)=915 cm^{-1}, δ(SiH)=663 cm^{-1}, δ(SiH_2)=626 cm^{-1}. Independently of the method used for hydrosilylation, the IR profiles are similar with a slight variation of ±3 cm^{-1}. In addition, the vibrational stretching mode for Si–C is expected to appear in the range of 680–760 cm^{-1} [17]. Because the Si–H_x stretching mode around

Table 1 Two-pot route for functionalization of silicon nanoparticles

Sample	Ligand	Method	Time, temperature	I(Si–O)/I(Si–H)	I(C–H)/I(Si–H)	E_h
A	1-Octene	Thermal	4 h at 80 °C	0.74	0.55	10
B	1-Octene	Platinum catalyst	4 h at 80 °C	4.21	1.85	61
C	1-Octene	Ph_3C^+	4 h at 80 °C	0.66	0.88	8
D	1-Octene	AIBN	4 h at 80 °C	0.89	1.37	13
E	1-Octene	UV light	4 h at 25 °C	0.86	0.42	5
F	1-Octene	Thermal	4 h at 140 °C	0.82	0.53	13

2,100 cm^{-1} becomes substantially broadened and in some cases featureless after hydrosilylation, it could not be determined whether the reaction exhibits any selectivity with respect to the Si–H_x functionalities.

The data in Table 1 allow a comparison of the reaction efficiencies under the assumption that the intensities of the different Si–H_x bonds are approximately the same. Different methods lead to consistent variation in the amount of decrease, suggesting that the efficiency of the reaction is strongly related to method used.

According to reference [18], the thermally supported reaction is assumed to pass through a four-centered complex between hydrogen bound to silicon and the two carbon atoms of the alkylene group (Scheme 1a), yielding an efficiency E_h of 10%. An increase in temperature to 140 °C gives only a small increase in efficiency (13%; sample F in Table 1) accompanied by a small increase in oxidation. The highest efficiency of 61% was achieved when platinum was used as a catalyst. This is in accordance to the general experimental finding that platinum complexes are extremely effective catalysts for the hydrosilylation of alkenes with molecular silanes in solution [19] as well as for the alkylation of Si(100) surfaces [20]. At the same time, it was found that the platinum complex could also catalyze the oxidation of the silicon surface. This is also reflected in our experiment, where a new Si–H band, assigned to an oxide-back-bonded Si–H stretching mode, appears at 2,260 cm^{-1}. This indicates that functionalization is accompanied by significant oxidation of the silicon surface, whereas the highest I(Si–O)/I(Si–H) is observed when platinum is used as a catalyst.

Lewis acid (Ph_3C^+)-mediated hydrosilylation requires nucleophilic attack by the 1-alkene of a surface silicon-based positive charge and subsequent hydride abstraction from an additional equivalent of silane. This results in the silylated alkane product as outlined in Scheme 1b. The silylenium cation is formed through hydride abstraction with the triphenylcarbenium cation via Corey hydride transfer [21, 22].

Lewis acid hydrosilylation reaction was done using $EtAlCl_2$ [23], carbenium ions [24] or boranes [25]. The ability of the Lewis acid to annihilate traces of water, which could otherwise add across weak Si–Si bonds, is almost certainly an important factor in reducing competing, concomitant oxidation. But still a little oxidation is noted in these reactions (Fig. 2c) in our case.

In case of the radical-mediated hydrosilylation, an initiator (in our case AIBN) undergoes homolytic cleavage to form a radical (Scheme 2b). This radical can then abstract the hydrogen atom from a surface Si–H group to produce a silicon radical. Because silyl radicals are known to react extremely rapidly with olefins, formation of a silicon carbon bond is the next probable step. The carbon-based radical can then abstract a hydrogen atom either from a neighboring Si–H group or from the allylic position of a non-reacted olefin. With AIBN, the hydrosilylation efficiency in our experiment was 13%.

The lowest hydrosilylation efficiency was obtained in the photochemical reaction induced by UV light. It is described in the literature that UV light can promote hydrosilylation of unsaturated compounds due to homolytic cleavage of Si–H bonds [11]. In the hydrosilylation reaction, a crucial step is the formation of the silicon surface radicals. The minimal energy needed for Si–H bond homolysis in solution appears to be 3.5 eV (338 kJ mol^{-1}, when the silicon atom is bonded to three other silicon atoms), requiring wavelengths shorter than 350 nm. UV light illumination induces homolytic Si–H cleavage to produce silicon radicals, followed by a radical chain mechanism. Figure 2e shows the strong effects of oxygen and UV light on the adsorption of 1-octene.

The efficiency of hydrosilylation for thermally, radically or Lewis acid- mediated hydrosilylation on silicon nanoparticles surfaces are comparable (see Table 2).

At the same time, the thermally mediated hydrosilylation (samples G and H) as compared to radical (sample I)- or carbocation (sample J)-mediated hydrosilylation led to the comparable results concerning the highest I(C–H_x)/I(Si–H_x) but at the same time to the lowest I(Si-O)/I(Si-H_x). The oxidation of the H-terminated surface competes with the hydrosilylation and is thermodynamically favoured, as the Si–H and Si–C bonds have a binding energy of 323 and 306 kJ mol^{-1}, respectively, whereas the Si–O bond with 444 kJ mol^{-1} is significantly stronger [11]. According

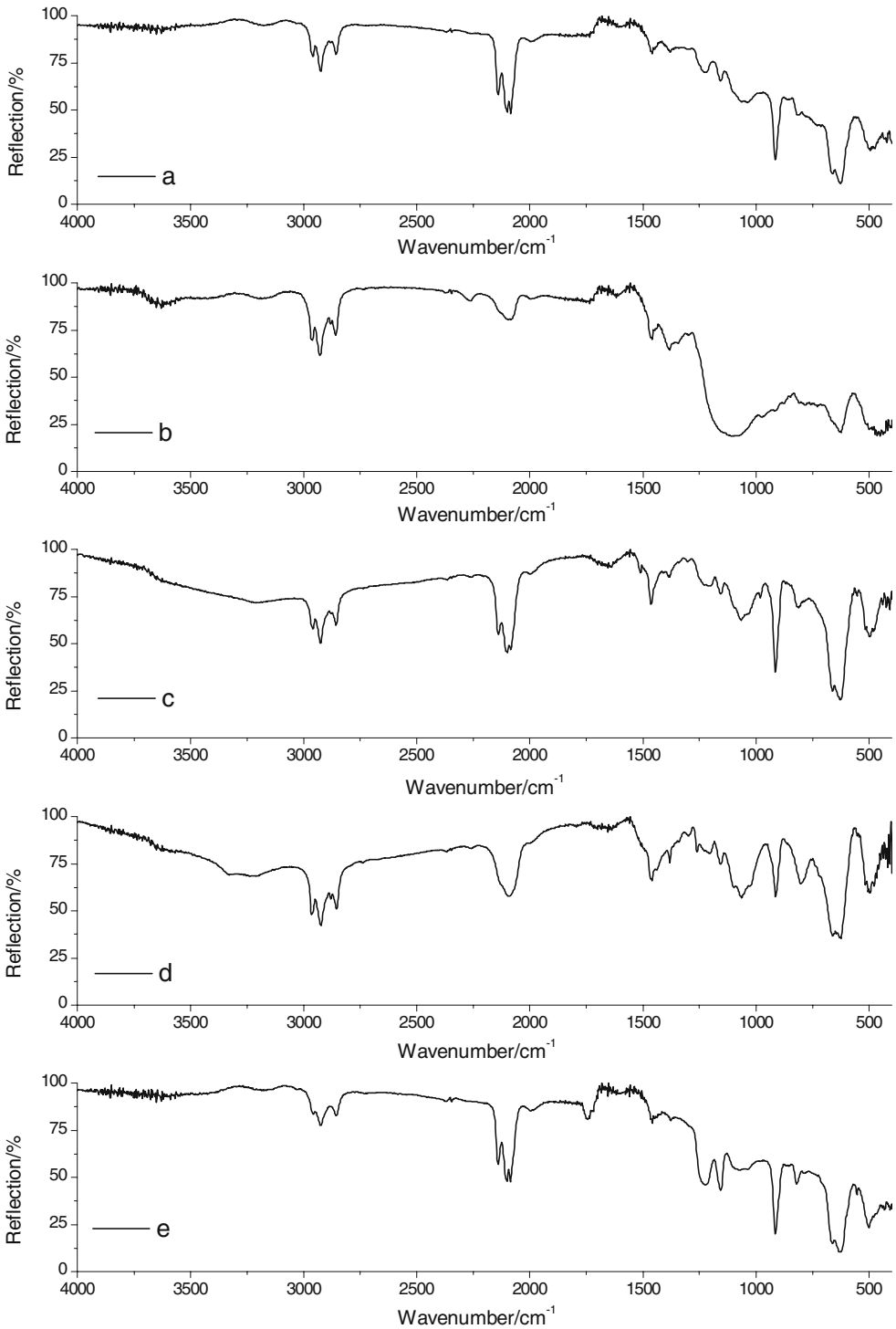

Fig. 2 DRIFT spectra of hydrogen-terminated silicon nanoparticles obtained upon different mediated hydrosilylation with 1-octene: **a** thermally, **b** with platinum-1,3-divinyl-1,1,3,3-tetramethyldisiloxan-complex, **c** with triphenylcarbenium-tetrakis (pentafluorophenyl)borate, **d** with AIBN, **e** by UV light

to the Polanyi–Hammond postulate, a surface modification with ionic or radical character, e.g. with water or oxygen, should be significantly faster then the reaction with the 1-alkene (*product development control*) [26]. The reaction rate is proportional to the base strength of the affecting species (Scheme 2). A surface modification with non-polar character like the thermally induced hydrosilylation shows barely side reactions because of the concerted reaction process. The reaction of the H-terminated surface with water and oxygen then seems to be kinetically inhibited.

To suppress the oxidation, another method was chosen, i.e. one-pot route. To give an impression of the nanoparticles we obtained with this method, Fig. 3 shows some images. A number of individual 20-nm nanoparticles as

Scheme 1 Reaction of hydrogen-terminated silicon nanoparticles with 1-alkenes. **a** Thermal activation. **b** Radical activation

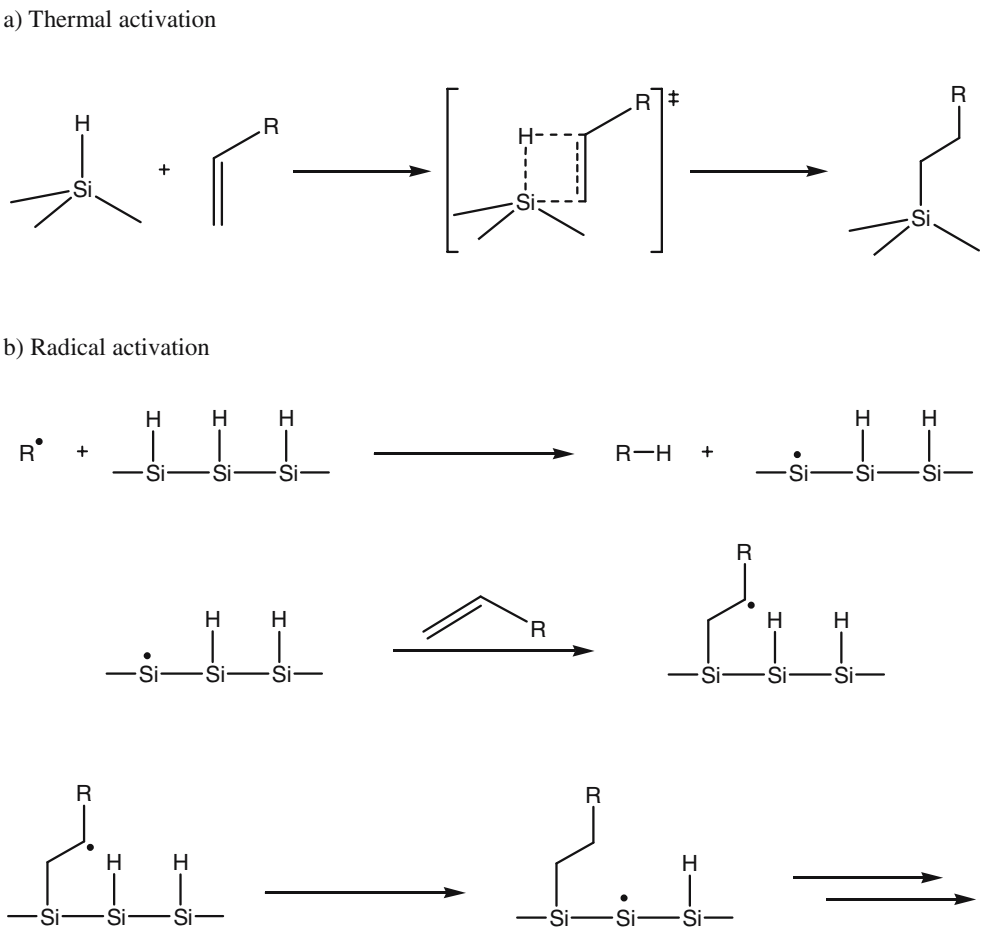

well as some aggregates can be seen. High-resolution TEM (Fig. 3b) indicates a high crystallinity of the silicon nanoparticles and also the formation of grain boundaries, which are amorphous with an average thickness of about 0.8 nm.

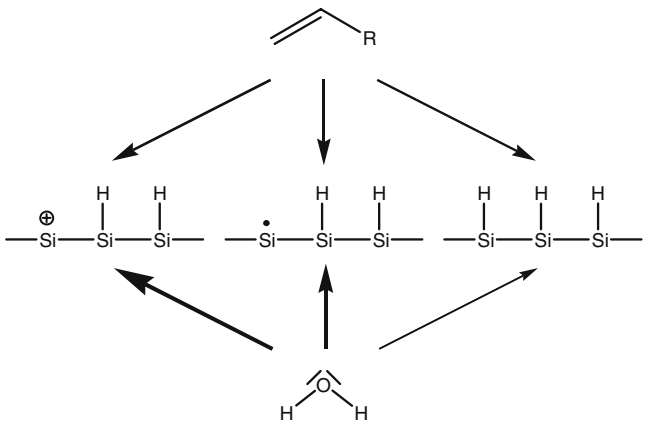

Scheme 2 Water and 1-alkene compete for the bonding with hydrogen-terminated silicon. The *arrow strength* denotes the reaction rate of the respective modification

We previously defined the term efficiency of hydrosilylation, but in this case, we do not know the intensity of Si–H_x before hydrosilylation. When we directly compare the FTIR spectrum of silicon nanoparticles modified with 1-octene obtained by two-pot route and one-pot route, the efficiency of hydrosilylation appears to be higher. The intensity of the $\nu_{as}(CH_2)$ stretching mode at 2,922 cm^{-1} compared with the intensity of ν(Si–H_x) at 2,100 cm^{-1} in case of one-pot route [sample G I(C–H_x)/I(Si–H_x)=0.93] is almost two times higher than in case of two-pot route [sample A I(C–H_x)/I(Si–H_x)=0.55]. Because the physisorption of free alkenes [ν=1,650 cm^{-1} (C=C) or ν= 3,050 cm^{-1} (C=CH_2)] is not evident, the increase in the intensity $\nu_{as}(CH_2)$ is caused by hydrosilylation. It is also important to note that in case of the one-pot route, the intensity of ν(Si–O) band at 1,096 cm^{-1} is smaller than in case of the two-pot route. The reason of this might be that in the thermally mediated one-pot route, silicon nanoparticles are, during the entire reaction, in contact with hydrofluoric acid. Song et al. [27] have shown that after treatment of the freshly etched, hydrogen-terminated porous silicon with phenyllithium and subsequent air hydrolysis, the infrared spectrum exhibits band characteristic

Table 2 One-pot route for functionalization of silicon nanoparticles

Sample	Ligand	Method	Time, temperature	I(Si–O)/I(Si–H)	I(C–H)/I(Si–H)
G	1-Octene	Thermal	4 h at 80 °C	0.59	0.99
H	1-Octene	Thermal	114 h at 80 °C	0.57	0.93
I	1-Octene	Ph_3C^+	23 h at 60 °C	1.17	1.52
J	1-Octene	DBPO	15 h at 60 °C	0.43	0.48
K	1-Hexadecene	Thermal	2 h at 100 °C	1.36	2.11
L	1-Hexadecene	Thermal	17 h at 120 °C	1.23	1.92
M	1-Hexadecene	Ph_3C^+	20 h at 40 °C	1.64	1.51
N	1-Hexadecene	Platinum catalyst	4 h at 40 °C	3.98	3.17

of silicon-bound phenyl groups accompanied with a strong and broad silicon oxide stretching mode at 1,100 cm^{-1}. The data indicate that functionalization is accompanied by significant oxidation of the silicon surface. This surface oxide can be removed by exposure of the sample to hydrofluoric acid (40%)/ethanol (1:1). After this treatment, there was no concomitant loss in intensity of the ν(C–H) and ν(C–C) IR bands associated with the phenyl group, indicating that the hydrofluoric acid (40%)/ethanol (1:1) leaves this species intact on the silicon surface. In the thermally mediated one-pot route, the hydrofluoric acid continuously removes surface oxide but the allyl group stays bound to the surface.

To investigate the influence of the different mediated hydrosilylation reactions in the one-pot route and influence of ligand length, we replaced 1-octene in all reactions with 1-hexadecene. The results are shown in Table 2. To summarize, the hydrosilylation reaction produces the best results accordingly: higher I(C–H_x)/I(Si–H_x) and lower I(Si–O)/I(Si–H_x) if it is performed thermally. A substantial oxidation was also noted even if considerable precautions were taken. The increase in reaction time does not increase the ratio I(C–H)/I(Si–H_x). The results agree with the work of Gurtner et al. [28], who has shown that, for functionalization of the hydrogen-terminated porous silicon with halogenide, the intensity of ν(C–H_x) absorption approaches a constant value already after 60 s. In contrast to Si(111) surfaces, we did not see any hints on a chain length dependence in the efficiency, presumably due to the low surface coverage and/or due to the structurally disordered and faceted surface of the nanoparticles.

Conclusion

In conclusion, we compared the thermal-, radical-, carbocation- and UV light-mediated hydrosilylation of silicon nanoparticles and showed that each reaction took place. The efficiency of hydrosilylation for thermal-, radical- and Lewis acid-mediated hydrosilylation on silicon nanoparticles surfaces, deduced from the intensity of the ν(Si–H) absorption, are comparable. Water and 1-alkene compete for the bonding with hydrogen-terminated silicon, but the thermally induced hydrosilylation shows barely side reactions because of the concerted reaction process. The reaction of the hydrogen-terminated surface with water and oxygen then seems to be kinetically inhibited.

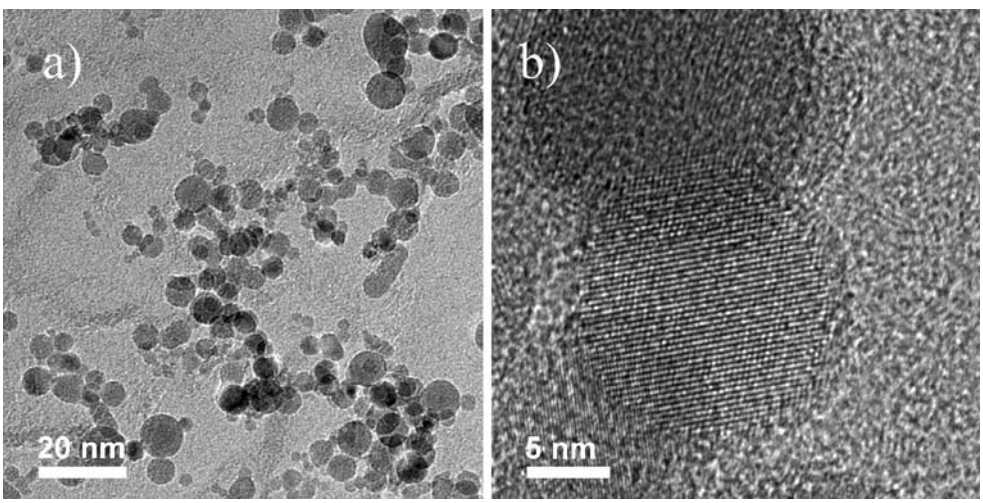

Fig. 3 **a** Bright-field scanning transmission electron microscopy (STEM) image and **b** high-resolution TEM micrograph of octane-terminated silicon nanoparticles obtained from the one-pot route

Acknowledgment This project is co-financed by the European Union and is financially supported by the state of North Rhine-Westphalia in Germany. The authors would like to thank Christian Brinkmöller for his support.

References

1. Buriak JM (1999) Chem Commun 12:1051
2. Hirschman KD, Tsybeskov L, Duttagupta SP, Fauchet SP (1996) Nature 384:338
3. Sailor MJ, Lee EJ (1997) Adv Mater 9:783
4. Lee EJ, Bitner TW, Ha JS, Shane MJ, Sailor MJ (1996) J Am Chem Soc 118:5375
5. Linford MR, Fenter P, Eissenberger PM, Chidsay CED (1995) J Am Chem Soc 117:3145
6. Sieval AB, Demirel AL, Nissink JWM, Linford MR, Maas J, Jeu WHD, Zuilhof H, Sudholter EJR (1998) Langmuir 14:1759
7. Buriak JM, Stewart MP, Geders TW, Allen MJ, Choi HC, Smith J, Raftery D, Canham LT (1999) J Am Chem Soc 121:11491
8. Li H-L, Fu AP, Fu DS, Guo GL, Gui LL, Tang YQ (2002) Langmuir 18:3198
9. Schmelzer JM, Lon AP, Stewart MP, Buriak JM (2002) Langmuir 18:2971
10. Wayner DD, Wolkow RA (2002) J Chem Soc Perkin Trans 2 (8):23
11. Buriak JM (2002) Chem Rev 102:1271
12. Wiggers H, Starke R, Roth P (2001) Chem Eng Technol 24:261
13. Higashi GS, Chabal YJ, Trucks GW, Raghavachari K (1990) Appl Phys Lett 56:656
14. Knipping J, Wiggers H, Rellingshaus B, Roth P, Konjhodzic D, Meier C (2004) J Nanosci Nanotech 4:1039
15. Hediger DHJ (1971) Infrarotspektroskopie. Akademische Verlagsgesellschaft, Frankfurt a M
16. Stewart MP, Robins EG, Geders TW, Allen MJ, Choi HC, Buriak JM (2000) Phys Status Solidi A 182:109
17. Pawlenko S (1986) Organosilicon chemistry. Walter de Gruyter & Co., Berlin
18. Cerofolini GF, Galati C, Reina S, Renna L (2003) Mater Sci Eng C 23:253
19. Lewis LN (1990) J Am Chem Soc 112:5998
20. Zazzera LA, Evans JF, Deruelle M, Tirrell M, Kessel CR, McKeown P (1997) J Electrochem Soc 144:2184
21. Corey JY (1975) J Am Chem Soc 97:3237
22. Lambert JB, Zhao Y, Zhang SM (2001) J Phys Org Chem 14:370
23. Buriak JM, Allen MJ (1998) J Am Chem Soc 120:1339
24. Schmeltzer JM, Porter LA, Stewart MP, Buriak JM (2002) Langmuir 18:2971
25. Katz HE (1985) J Org Chem 50:5027
26. Hammond H (1955) J Am Chem Soc 77:334
27. Song JH, Sailor MJ (1998) J Am Chem Soc 120:2376
28. Gurtner Ch, Wun AW, Sailor MJ (1999) Angew Chem 111:2132